Supplementary information

Current-induced restructuring in bent silver nanowires

Nitin M. Batra,[a] Ahad Syed,[b] and Pedro M. F. J. Costa [a]*

[a] King Abdullah University of Science and Technology, Physical Sciences and Engineering Division, Thuwal 23955-6900, Saudi Arabia

[b] King Abdullah University of Science and Technology, Core Labs, Thuwal 23955-6900, Saudi Arabia

* email: pedro.dacosta@kaust.edu.sa

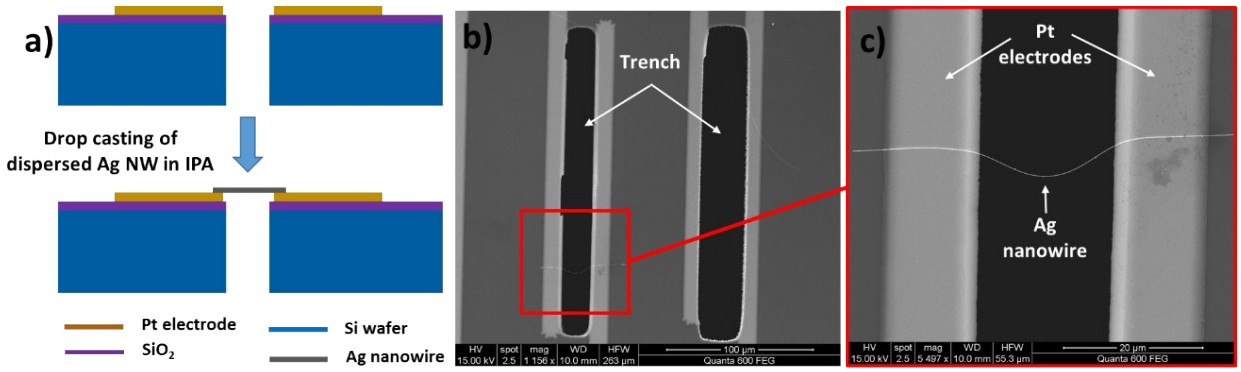

Figure S1 Sample preparation for in-situ TEM: a) Cross-sectional schematics of the custom-made chips and location of the suspended Ag nanowires; to place the nanowires, drops of a dispersion of these in IPA were casted onto the top-surface of the chips. b) Low-magnification SEM image showing a 0.25 x 0.25 mm section of an electrical TEM chip containing a suspended Ag nanowire. c) Magnified view of the boxed area in b); both the Pt electrodes and a bent Ag NW bridging them are visible. The Ag NW was >50 µm long and the contact to the Pt electrodes was sustained by surface forces; the trench width was around 20 µm, while the total length of contact between the Ag NW with each of the Pt electrodes was 25-30 µm. Note: when more than one nanowire was crossing a trench, a focused ion or laser beam was used to isolate an individual interconnect.

Supplementary information

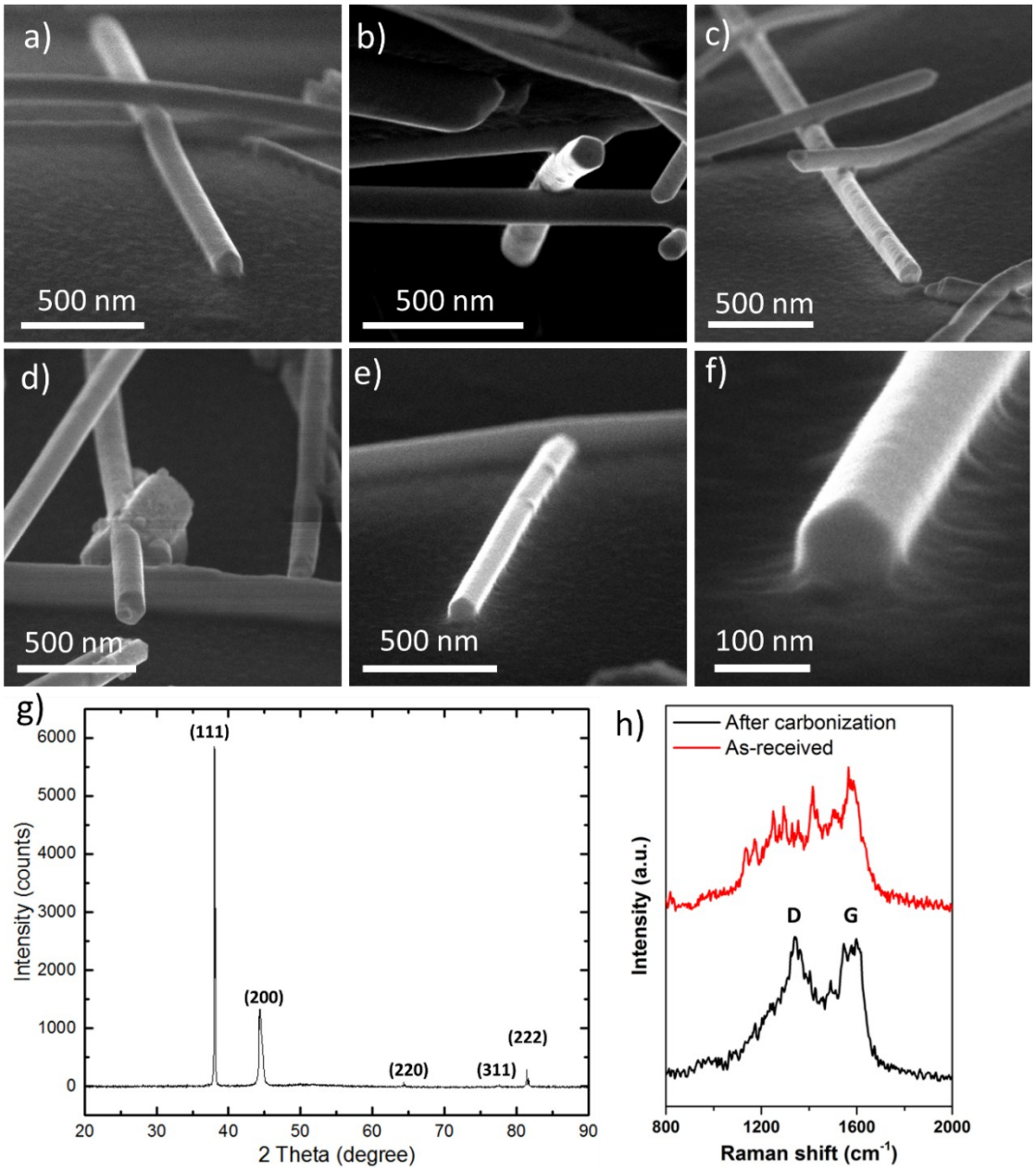

Figure S2 Characterisation of the as-received Ag NW: a-e) SEM images of the nanowires in cross-section (acquired with a stage tilt of 60-80°). f) High magnification SEM image of the penta-twinned nanowire in e). g) Powder XRD pattern of the Ag sample; comparison with the JCPDS data card (file no. 04-783) shows that all peaks can be assigned to a face-centered cubic (*fcc*) Ag structure, the sharp peaks at 38° and 44° are assigned to (111) and (200), respectively; this corroborates the TEM results of a <110> growth direction (Ag NW with a penta-twinned structure means that a single nanowire consisted of five *fcc* crystals joined at {111} twinned facets and [110] edges)[1-4]. h) Raman spectra of the Ag NW sample, before and after exposure to the laser beam; the window of frequencies selected corresponds to the region where the characteristic D-

Supplementary information

and G-bands of carbon materials are observed; in the as-received state (red line), there is number of overlapping bands that are assigned to a polymer-type profile (the exact nature of the coating was not disclosed by the vendor but we infer it to be PVP); using the laser as a high-energy beam (note that the power was increased from that normally used for spectroscopy measurements), the organic coating carbonized and its spectrum changed considerably (black line); the sample was prepared by drop casting a suspension of the nanowires onto a Si wafer.

Table S1 Dimensions, electrical resistance and resistivity of the Ag nanowires

NW #	Diameter (nm)	Length (μm)	Resistance (Ω)	Resistivity (Ω-m)
1	110	17	370	2.1E-07
2	175	13	305	5.6E-07
3	300	22	285	9.2E-07
4	98	12	467	2.9E-07
5	85	20	560	1.6E-07
6	120	22	520	2.7E-07
7	85	30	320	5.0E-08
8	75	16	650	1.8E-07
9	117	32	332	1.1E-07
10	146	17	350	3.4E-07
11	97	13	462	2.6E-07
12	128	14	394	3.6E-07
13	70	10	1542	5.9E-07
14	140	26	367	2.2E-07
15	116	12	381	3.4E-07
16	122	30	306	1.2E-07
17	110	27	365	1.3E-07
18	120	18	200	1.3E-07
19	115	22	500	2.4E-07
20	120	10	386	4.4E-07
21	129	14	285	2.7E-07
22	173	18	340	4.4E-07
23	143	15	278	3.0E-07
24	121	25	346	1.6E-07
25	142	20	660	5.2E-07
26	150	19	500	4.6E-07
27	83	18	860	2.6E-07
28	135	25	412	2.4E-07

Supplementary information

Table S2 Comparison with literature (chronologically ordered): coating, dimensions, resistivity and probing processes of Ag NW

Reference	Coating layer	Diameter (nm)	Length (µm)	Resistivity (Ω-m)	2-probe (2p) or 4-probe (4p) measurements
Wiley et al., (2006) [5]	PVP	45	4	1.1E-07	2p
Liu et al., (2008) [6]	PVP	28	1	4.3E-07	2p
Xu et al., (2009) [7]	PVP	200	23	1.6E-08	4p
Bernal et al., (2014) [8]	PVP	77	3-7	2.0E-07	2p
Cheng et al., (2015) [9]	n.d. (commercial)	227	27	7.9E-08	2p
Wang et al., (2018) [10]	PVP	97	15	4.2E-08	2p
This work	n.d. (commercial)	70-300	10-32	3.1E-07	2p

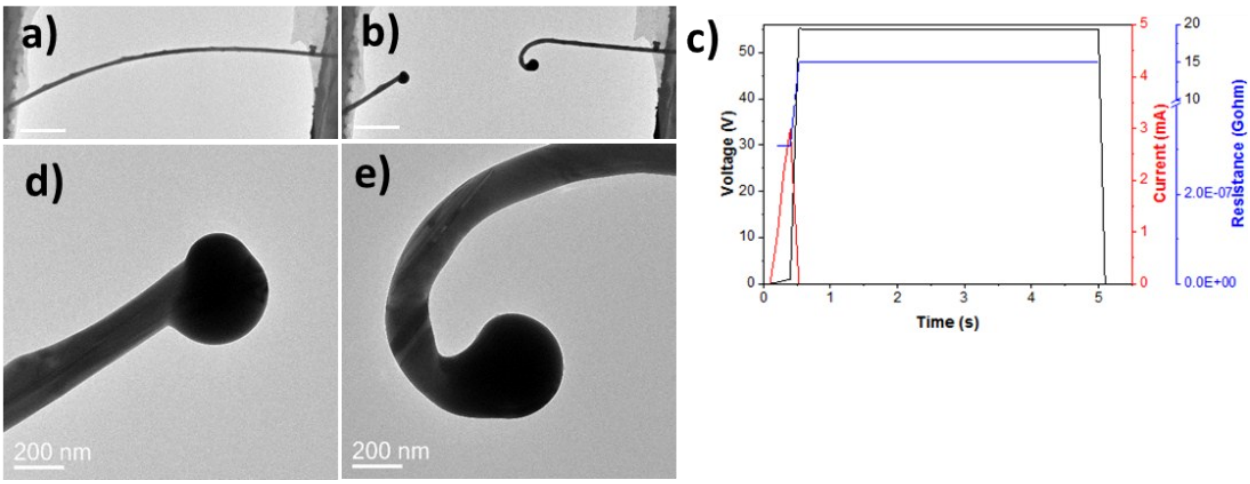

Figure S3 Fast-rate breakdown of a (almost) straight Ag nanowire (NW-2): a) and b) Low magnification TEM micrographs of the Ag NW-2, before and after breakdown, respectively. c) Voltage vs. time curve with output datasets of current and resistance. d) and e) High magnification TEM micrographs of the Ag NW-2 segments, after breakdown.

The Ag NW-2 (length: 13 µm, diameter: 175 nm) was subjected to several cycles of incremental bias (fast rate, >20 mV/s), with the threshold of current being raised at each cycle (i.e. ramping up from 0.5 to 5 mA). During the last cycle, the device failed within a fraction of a second and at a current of 3 mA (**Fig. S3c)**. Interestingly, the resistance of this device (305 Ω) did not change for current thresholds of <2.5 mA. When the rate of current flowing through the two-terminal device was very high, resistive (or Joule) heating took place. In the present case, a hot-spot developed at approximately mid-length of the nanowire. Eventually, with the continuous increase in

temperature, the melting point of the Ag nanostructure was reached and the wire broke abruptly (**Video 1**). This resulted in two separate segments with "drop-like" ends (**Figs. S3d-e**).

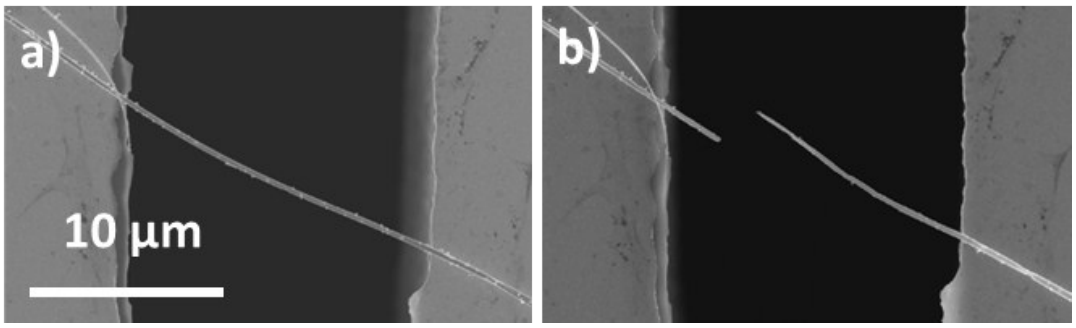

Figure S4 Slow-rate breakdown of a straight Ag nanowire (NW-3): a) and b) SEM images of the NW-3 (as described in the main text) before and after breakdown, respectively. It is clear that sectioning took place nearer one of the electrodes, not at the mid-length of the interconnect.

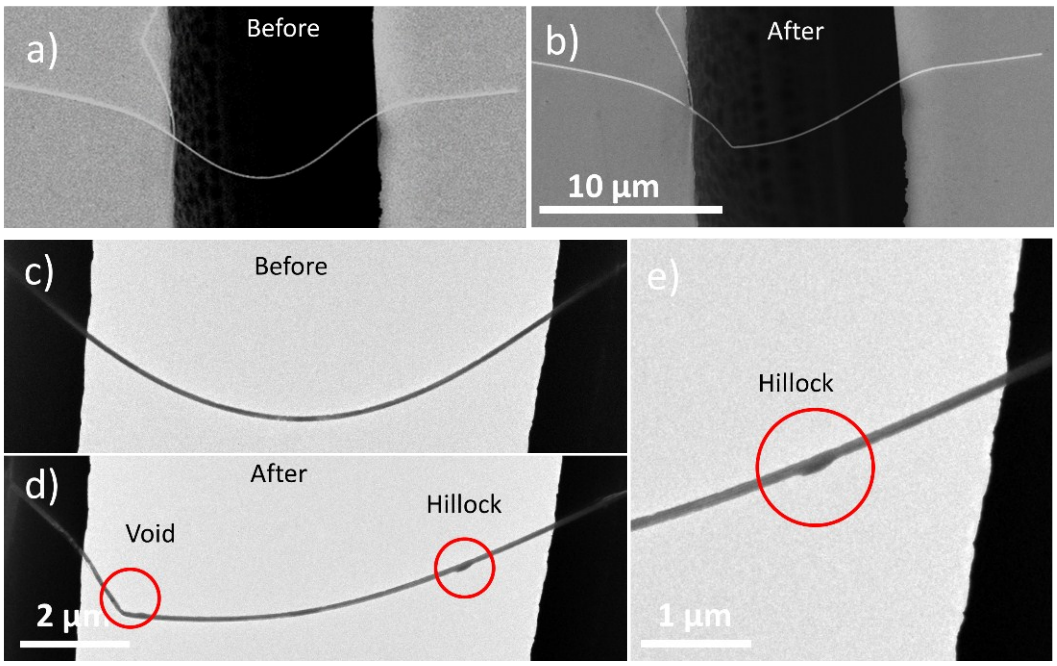

Figure S5 Breakdown of a bent Ag NW (buckling, NW-4): a) and b) SEM images of the NW-4 before and after buckling, respectively. c) and d) Corresponding TEM micrographs of a) and b), respectively; highlighted in d) are the formation of a void and a hillock. e) High magnification TEM micrograph of the hillock marked in d).

Supplementary information

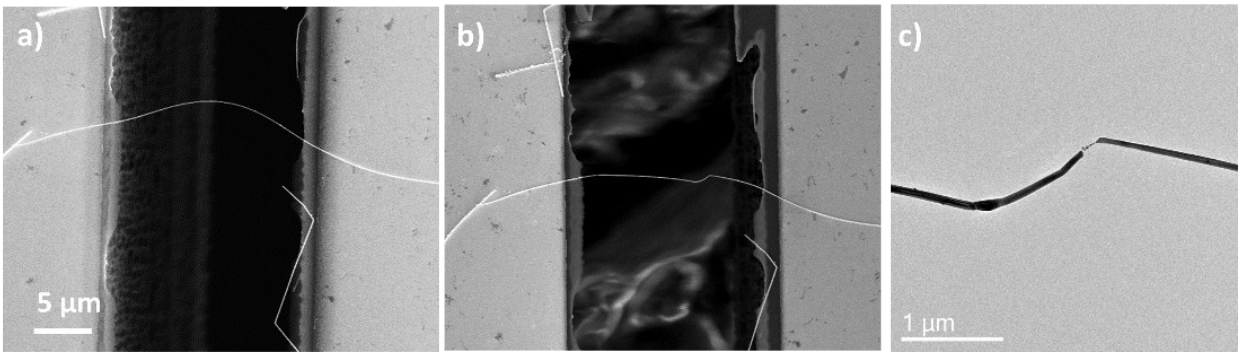

Figure S6 Breakdown of a bent Ag NW (buckling preceded by resonance, NW-5): a) and b) SEM images of the NW-5 before and after buckling, respectively. c) Corresponding TEM micrograph of the buckled region in b).

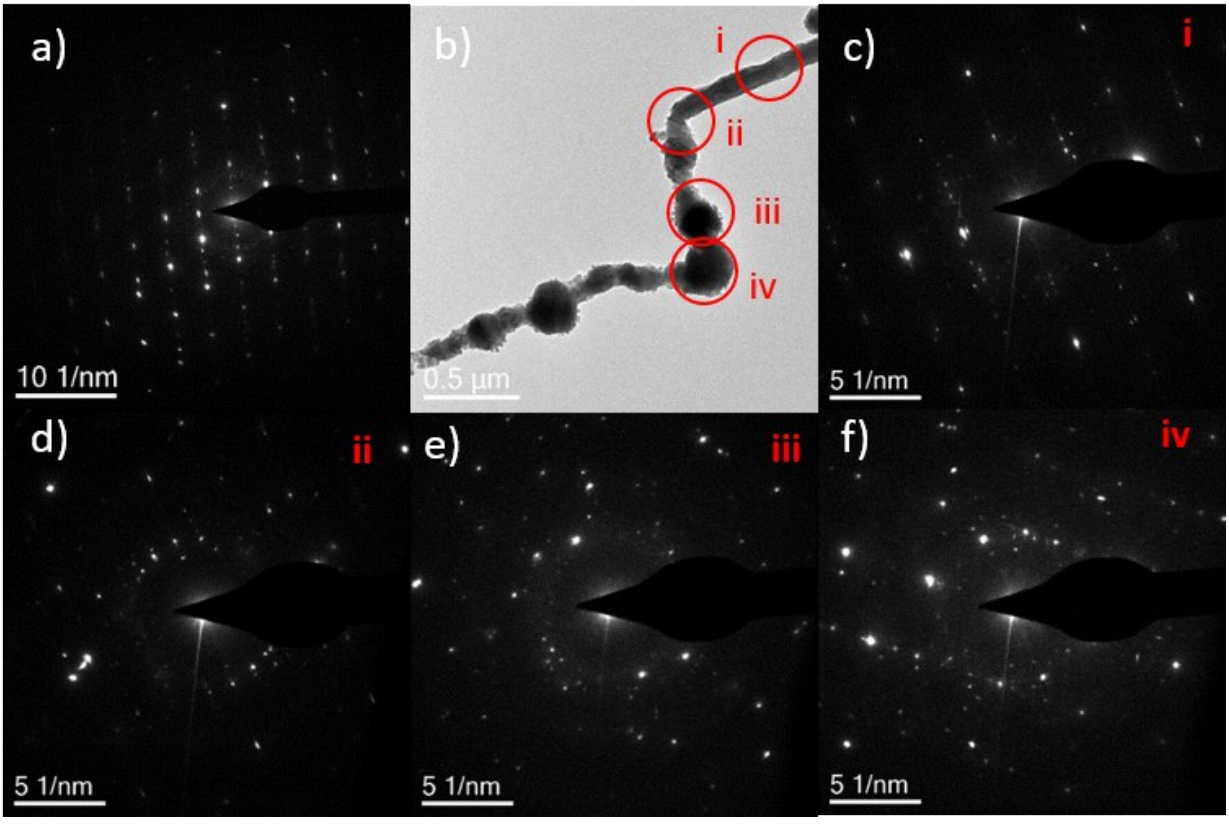

Figure S7 Breakdown of a bent Ag NW (buckling with retention of electrical function, NW-6): a) SAED pattern of the NW-6 in its initially crooked configuration. b) TEM micrograph, taken after restructuring, of the "knot-like" extended region; the red circles represent the area from where the SAED patterns shown in c) to f) were collected (also labelled with roman numbers). c)-f) SAED

patterns of the “knot-like” extended region, the multigrain-like nature of this nanowire section is notable.

Video-recording

Video 1: “Drop-like” breakdown under fast bias in NW-2.

Video 2: “Needle-like” breakdown under slow bias in NW-3.

Video 3: Buckling and failure of NW-4.

Video 4: Resonance and elastic deformation in NW-5 during 1st cycle.

Video 5: Buckling and plastic deformation in NW-5 during 2nd cycle.

Video 6: Buckling with retention of electrical function in NW-6.

Video 7: Buckling and resonance with retention of electrical function in NW-7.

References

1. H. Chen, Y. Gao, H. Zhang, L. Liu, H. Yu, H. Tian, S. Xie and J. Li, *Journal of Physical Chemistry B*, 2004, **108**, 12038-12043.
2. J.-J. Zhu, C.-X. Kan, J.-G. Wan, M. Han and G.-H. Wang, *Journal of Nanomaterials*, 2011, **2011**, 1-7.
3. Y. Gao, P. Jiang, D. F. Liu, H. J. Yuan, X. Q. Yan, Z. P. Zhou, J. X. Wang, L. Song, L. F. Liu, W. Y. Zhou, G. Wang, C. Y. Wang and S. S. Xie, *Chemical Physics Letters*, 2003, **380**, 146-149.
4. Y. Sun, Y. Ren, Y. Liu, J. Wen, J. S. Okasinski and D. J. Miller, *Nat Commun*, 2012, **3**, 971.
5. B. J. Wiley, Z. Wang, J. Wei, Y. Yin, D. H. Cobden and Y. Xia, *Nano Letters*, 2006, **6**, 2273-2278.
6. X. Liu, J. Zhu, C. Jin, L. M. Peng, D. Tang and H. Cheng, *Nanotechnology*, 2008, **19**, 085711.
7. W. Xu and S. H. Yu, *Small*, 2009, **5**, 460-465.
8. R. A. Bernal, T. Filleter, J. G. Connell, K. Sohn, J. Huang, L. J. Lauhon and H. D. Espinosa, *Small*, 2014, **10**, 725-733.
9. Z. Cheng, L. Liu, M. Lu and X. Wang, *Scientific Reports*, 2015, **5**, 10718.
10. J. Wang, Z. Wu, C. Mao, Y. Zhao, J. Yang and Y. Chen, *Scientific Reports*, 2018, **8**, 4862-4869.